Cellular/Molecular

Slack and Slick K_{Na} Channels Regulate the Accuracy of Timing of Auditory Neurons

Bo Yang,[1] Rooma Desai,[1] and Leonard K. Kaczmarek[1,2]

Departments of [1]Pharmacology and [2]Cellular and Molecular Physiology, Yale University School of Medicine, New Haven, Connecticut 06520

The *Slack* (sequence like a calcium-activated K channel) and *Slick* (sequence like an intermediate conductance K channel) genes, which encode sodium-activated K^+ (K_{Na}) channels, are expressed at high levels in neurons of the medial nucleus of the trapezoid body (MNTB) in the auditory brainstem. These neurons lock their action potentials to incoming stimuli with a high degree of temporal precision. Channels with unitary properties similar to those of Slack and/or Slick channels, which are gated by $[Na^+]_i$ and $[Cl^-]_i$ and by changes in cytoplasmic ATP levels, are present in MNTB neurons. Manipulations of the level of K_{Na} current in MNTB neurons, either by increasing levels of internal Na^+ or by exposure to a pharmacological activator of Slack channels, significantly enhance the accuracy of timing of action potentials at high frequencies of stimulation. These findings suggest that such fidelity of timing at high frequencies may be attributed in part to high-conductance K_{Na} channels.

Key words: **Na^+-activated K^+ (K_{Na}) channels; medial nucleus of the trapezoid body (MNTB); patch clamp; computer simulations; synaptic transmission; immunohistochemistry**

Introduction

The brainstem binaural auditory pathway computes the localization of a sound source by comparing the relative phase (interaural time differences) and volume (interaural intensity differences) of sound stimuli received at each cochlea. For this pathway to function efficiently, it is essential that its component neurons are able to preserve the precise timing information contained within the auditory signal. In mammals, globular bushy neurons of the anterior ventral cochlear nucleus (aVCN) and principal neurons in the medial nucleus of the trapezoid body (MNTB) are capable of firing action potentials that are faithfully locked to the phase of incoming stimuli at frequencies up to ~600 Hz (Brownell, 1975; Banks and Smith, 1992; Wu and Kelly, 1993; Taschenberger and von Gersdorff, 2000). MNTB neurons are important relay elements that receive a secure synaptic input from the contralateral aVCN via the calyx of Held (Lenn and Reese, 1966; Morest, 1968, 1973; Forsythe and Barnes-Davies, 1993) and send an inhibitory projection to the ipsilateral medial superior olive (MSO) and lateral superior olive (LSO). Both the MSO and LSO also receive direct excitatory projections from the aVCN. The binaural pathway has a number of important adaptations to preserve the fidelity of action potential timing, including two giant excitatory synapses (the endbulb and the calyx of Held), postsynaptic receptors with fast kinetics (Barnes-Davies and Forsythe, 1995; Isaacson and Walmsley, 1995), low-threshold Kv1 family potassium currents that suppress multiple action potential generation during the decay of synaptic responses (Manis and Marx, 1991; Brew and Forsythe, 1995), and high-threshold Kv3 family potassium currents that minimize the action potential duration and allow high-frequency spike firing (Wang et al., 1998; Song et al., 2005).

The significance of K^+ conductances in the regulation of neuronal excitability and their involvement in neuronal pathologies has been well documented (Hille, 2001; Levitan and Kaczmarek, 2002). K^+ channels encoded by the *Slack* (*Slo*2.2; sequence like a calcium-activated K channel) and *Slick* (*Slo*2.1; sequence like an intermediate conductance K channel) genes are gated by intracellular Na^+ ($[Na^+]_i$) and Cl^- ($[Cl^-]_i$), and these channels are present in the brain regions (Bhattacharjee et al., 2002, 2005) reported to possess sodium-activated K^+ (K_{Na}) channels (Egan et al., 1992; Dryer, 1994). Nevertheless, the physiological significance of these K_{Na} channel conductances in the CNS is still being clarified.

In this study, we have localized and identified K_{Na} channels in the principal neurons of the MNTB and have compared their properties with those of *Slack* and *Slick* expressed in oocytes and mammalian cell lines (Joiner et al., 1998; Bhattacharjee et al., 2003; Yuan et al., 2003; Santi et al., 2006; Yang et al., 2006). Current-clamp recordings from MNTB neurons and numerical simulations indicate that the activation of these K_{Na} channels allows temporal accuracy of firing to be increased at high frequencies of stimulation.

Materials and Methods

Electrophysiological recordings. Slices from postnatal day 10–13 (P10–P13) mice (129SV/EMS; The Jackson Laboratory, Bar Harbor, ME) were prepared as described previously (Barnes-Davies and Forsythe, 1995)

Received Sept. 27, 2006; revised Jan. 28, 2007; accepted Feb. 1, 2007.

This work was supported by National Institutes of Health Grants DC-01919 and NS42202 to L.K.K. B.Y. was supported by a Heritage Affiliate Postdoctoral Fellowship from the American Heart Association.

Correspondence should be addressed to Dr. Leonard K. Kaczmarek, Department of Pharmacology, 333 Cedar Street, Yale University School of Medicine, New Haven, CT 06520. E-mail: leonard.kaczmarek@yale.edu.

B. Yang's present address: Drug Discovery Support, Boehringer Ingelheim Pharmaceuticals, Ridgefield, CT 06877-0368.

DOI:10.1523/JNEUROSCI.5308-06.2007

 0270-6474/07/272617-11$15.00/0

and transferred to a recording chamber that was perfused continuously (1 ml/min) with artificial CSF (ACSF) (in mM: 125 NaCl, 2.5 KCl, 26 $NaHCO_3$, 1.25 NaH_2PO_4, 2 sodium pyruvate, 3 *myo*-inositol, 10 glucose, 2.0 or 0.5 $CaCl_2$, and 1 $MgCl_2$ gassed with 95% O_2/5% CO_2, pH 7.4, at 21–23°C). Whole-cell recordings (Hamill et al., 1981) were made from visually identified MNTB principal neurons using an EPC-7 amplifier (HEKA Elektronik, Lambrecht, Germany) for voltage-clamp recordings and an Axoclamp-2A amplifier in the bridge-balance mode for current-clamp recordings (Magistretti et al., 1996). All of the experiments were performed at room temperature (RT; 21–22°C). Electrodes for whole-cell recordings had a resistance of 2–4 MΩ when filled with an intracellular solution containing the following (in mM): 97.5 potassium gluconate, 32.5 KCl, 5 EGTA, 10 HEPES, and 1 $MgCl_2$, pH 7.2. When $[Na^+]_i$ was varied, NMDG (*N*-methyl-D-glucamine) was used as the substitute. For voltage-clamp recordings, TTX (1 μM) was also included in ACSF to block Na^+ currents (typically 5–10 nA at −20 mV). The series resistance for whole-cell recordings from MNTB neurons was <12 MΩ and compensated at 70–80%. No corrections were made for liquid-junction potentials. Data were filtered at 5 kHz and sampled at 10 kHz.

For channel recordings from excised patches in the inside-out configuration, the electrodes had resistances of ~7–9 MΩ when filled with the pipette solutions. Data were filtered at 5 kHz and sampled at 20 kHz for all protocols. The sign of the applied voltage refers to the bath with respect to the patch pipette. In every inside-out patch experiment, patches were excised from cells, and the membrane potential was stepped to 0 mV from a holding potential of −60 mV. For channel analysis, NP_o (N is the number of active channels, P_o is the open probability) was calculated using the single-channel search and event statistics algorithms in pClamp 9.0 software (Molecular Devices, Union City, CA). Averaged data are expressed as means ± SEM. Student's *t* test was applied for statistical analysis. A minimum *p* value of <0.05 was selected to determine significance. All values are plotted as means ± SEM.

Numerical simulations. Simulations were performed using previously described models of MNTB neurons (Liu and Kaczmarek, 1998; Wang et al., 1998; Richardson and Kaczmarek, 2000; Macica et al., 2003; Song et al., 2005) and of *Slick* and *Slack* currents (Bhattacharjee et al., 2005). Responses were simulated by integration of the following equation: $C\,dV/dt = I_{ext(t)} - I_{Na} - I_{Kv3.1} - I_{KvLT} - I_{KNa} - I_L$, where I_{Na} is the Na^+ current and $I_{Kv3.1}$ and I_{KvLT} are components of voltage-dependent K^+ currents. I_{KNa} is a K_{Na} with kinetic properties intermediate between those of *Slick* and *Slack*. I_L is the leak current, and stimuli $I_{ext(t)}$ were presented as step currents (0.2 ms) of 20–400 Hz. In Figure 9, *c* and *d*, $I_{ext} = 1.1, 1.1, 1.25$, and 1.4 nA for intracellular Na^+ levels of 0, 5, 20, and 40 mM, respectively. Equations for $I_{Kv3.1}$, I_{KvLT}, and I_L were identical to those described by Macica et al. (2003) and are based on fits to currents in MNTB neurons, as are those for I_{Na}, with the exception that E_{Na}, the reversal potential for Na^+ ions, was lowered from +50 to +45 mV and to +28 mV for simulations of 20 and 40 mM intracellular Na^+, respectively.

I_{KNa} was given by the equation $I_{KNa} = g_K n^2 s^4 (V + 80)$, where the variable *n* describes voltage dependence and is governed by equations identical to those for the other K^+ channels with the parameters $g_{KNa} = 0.06$ μS, $k_{\alpha n} = 0.141\ ms^{-1}$, $\eta_{\alpha n} = 0.0558\ mV^{-1}$, $k_{\beta n} = 0.0587\ ms^{-1}$, and $\eta_{\beta n} = 0.0308\ mV^{-1}$. These values provide kinetic behavior intermediate between that of *Slack* and *Slick* (Bhattacharjee et al., 2003). The parameter *s* is regulated by $[Na^+]_i$ and given by the following equation:

$$s = \frac{k_{fs}[Na_i]}{k_{bs} + k_{fs}[Na_i]},$$

with $k_{fs} = 0.14\ mM^{-1} ms^{-1}$ and $k_{bs} = 2.0\ ms^{-1}$.

The phase vector strength *V* in the model and in experimental data was calculated by the following equation:

$$V = \frac{1}{N}\sum_{i=1}^{i=N} \cos\left(2\pi \frac{D_i - \bar{D}}{P}\right),$$

where *N* is the number of action potentials evoked ($N > 1$), D_i is the delay time from onset of an individual stimulus pulse *i* to the peak of the action potential evoked by that pulse, $\bar{D}$ is the mean delay for all of the action potentials evoked by the train, and *P* is the period of the pulses during the train. Pulses that failed to generate action potentials were not included in the summation.

Immunohistochemistry. Brainstems of P11 mice were dissected out in ACSF at 0°C and fixed in 4% paraformaldehyde in PBS for 12 h at 4°C. The fixed tissue was cryoprotected at 4°C in PBS with a graded concentration of sucrose (4%, 30 min; 10%, 2 h; 15%, 2 h; 20%, 12 h). The tissue was frozen in optimal cutting temperature compound, and 8 μm transverse cryostat sections were cut at −21°C. The sections were stored on poly-lysine-coated slides at −80°C. For immunohistochemistry, the slides were rinsed in PBS for 5 min at RT and processed by the following: (1) blocking and permeabilization in PBS containing 10% goat serum

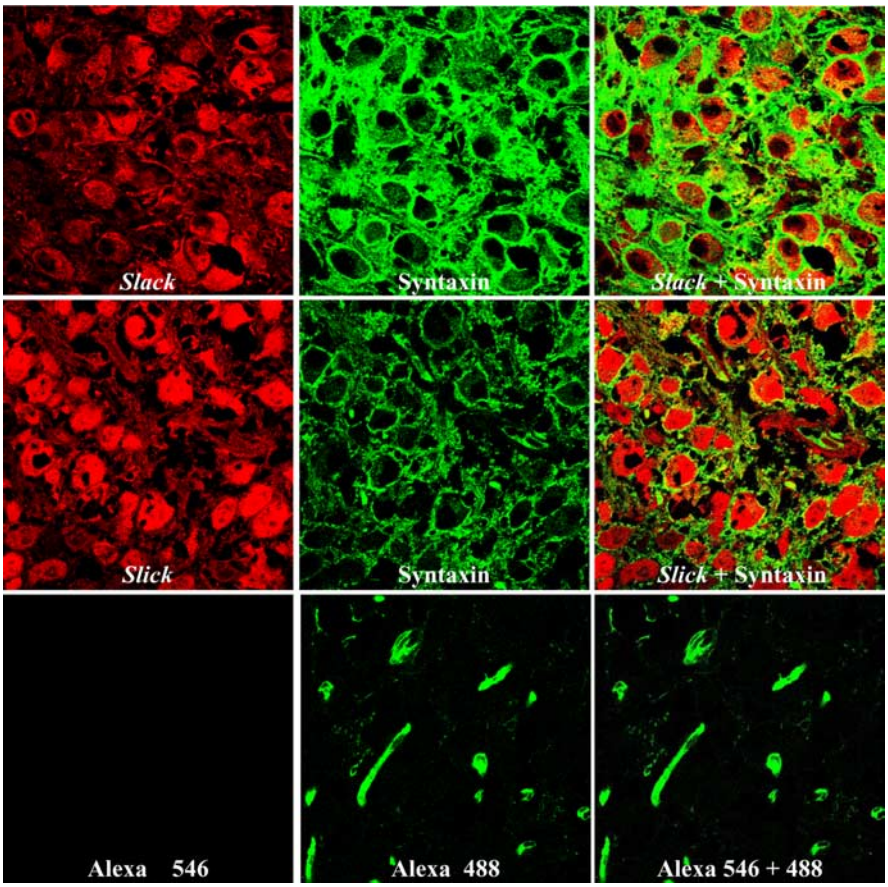

Figure 1. Slack and Slick subunits and K_{Na} channels are present in both the principal cells and the calyces of Held of the MNTB. Red signals show immunofluorescence for Slack (top row, left) and Slick (middle row, left) (detected with Alexa Fluor 546). Syntaxin immunofluorescence in the middle column is shown in green (detected with Alexa Fluor 488). Overlap of syntaxin with Slick or Slack immunoreactivity is shown in the right column. The bottom row shows a negative control with only the secondary antibodies.

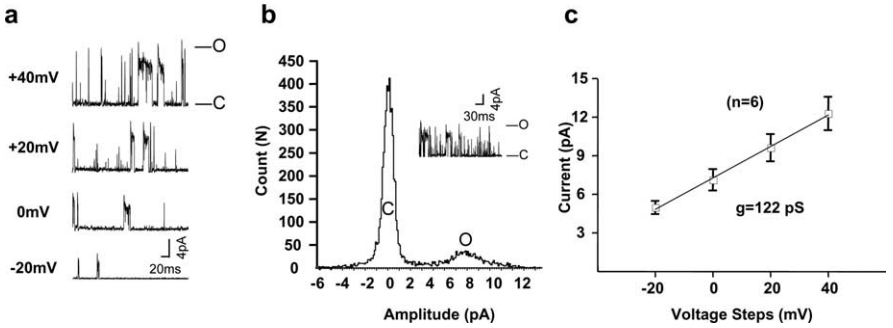

Figure 2. Traces of K_{Na} channel activity in patches excised from an MNTB neuron. ***a***, Recordings were acquired with voltage steps to −20, 0, +20, and +40 mV from a holding potential of −60 mV (with 130 mM $[K^+]_i$/2.5 mM $[K^+]_o$, 10 mM $[Na^+]_i$, 34.5 mM $[Cl^-]_i$). ***b***, Amplitude histogram of large-conductance channel activity evoked by a step from −60 to 0 mV with 130 mM $[K^+]_i$/2.5 mM $[K^+]_o$, 10 mM $[Na^+]_i$, 34.5 mM $[Cl^-]_i$. The inset shows current recording for this histogram. O, Open; C, closed. ***c***, Mean current–voltage (*I–V*) relationships of channels obtained by determining current amplitude at different voltages using histograms as in ***b*** ($n = 6$). The slope of the line fitted on this *I–V* plot gives a value of 122 pS.

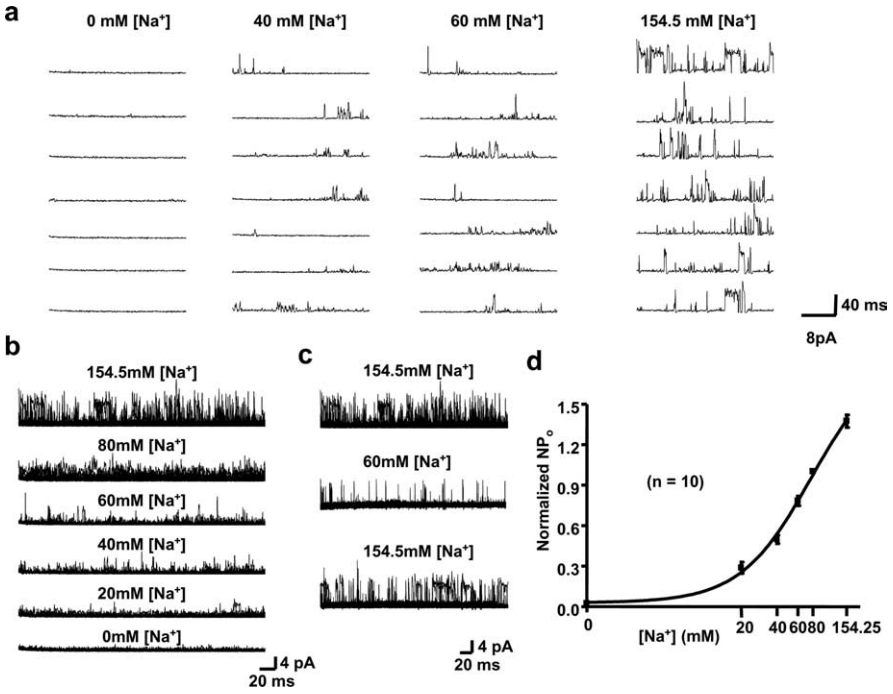

Figure 3. Gating of MNTB channels by $[Na^+]_i$. ***a***, Representative traces of channel activity in inside-out patches excised from principal neurons of the MNTB into a medium containing no Na^+ or containing 40, 60, or 154.5 mM $[Na^+]_i$ at the cytoplasmic face of the patch (with 130 mM $[K^+]_i$/2.5 mM $[K^+]_o$, 34.5 mM $[Cl^-]_i$). The membrane potential was stepped to 0 mV from a holding potential of −60 mV. ***b***, Na^+ dependence of channel gating demonstrated by superimposing 20 channel recordings from inside-out patches with $[Na^+]_i$ = 154.5, 80, 60, 40, 20, and 0 mM (with 130 mM $[K^+]_i$/2.5 mM $[K^+]_o$, 34.5 mM $[Cl^-]_i$). ***c***, Reversibility of the actions of $[Na^+]_i$. Records shown represent 20 superimposed channel traces from the same patch as in ***b***. After exposure of the patch to 154.5 mM $[Na^+]_i$ (top traces), $[Na^+]_i$ was lowered to 60 mM (middle traces) and returned to 154.5 mM (bottom traces). ***d***, Normalized NP_o values determined for different concentrations of Na^+ on the intracellular face of the membrane.

and 0.2% (wt/vol) Triton X-100 for 1 h, (2) application of primary antibodies in 100 μl of PBS containing 10% (wt/vol) goat serum and 0.2% Triton X-100 overnight at 4°C followed by 2 h at RT, (3) application of secondary antibodies in the same buffer as primary antibodies for 2 h at RT, and (4) mounting with the ProLong antifade kit (Invitrogen, San Diego, CA). Sections were washed with blocking buffer three times for 10 min between each step. Antibodies used were chicken polyclonal antibodies anti-*Slack* and anti-*Slick* (Bhattacharjee et al., 2002, 2005) and mouse monoclonal anti-syntaxin (diluted 1:200; Sigma, St. Louis, MO). The secondary antibodies were goat anti-mouse IgG conjugated with Alexa Fluor 488 (diluted 1:500; Invitrogen) and goat anti-chicken IgG conjugated with Alexa Fluor 546 (diluted 1:500; Invitrogen). Stained sections were viewed with a 63× water-immersion objective using confocal laser scanning microscopy. All of the images were acquired with identical settings.

Results

Slack and Slick channels are present in the principal neurons of the MNTB

Previous studies (Bhattacharjee et al., 2002, 2005) have demonstrated via *in situ* hybridization and immunohistochemistry that the mRNA and protein of both *Slack* (*Slo*2.2) and *Slick* (*Slo*2.1) genes, which encode Na^+-activated K^+ channels, are abundantly expressed in auditory brainstem nuclei such as the MNTB. To determine whether these K_{Na} channels are expressed in the principal neurons of the MNTB and/or in the presynaptic terminals of the calyces of Held, we performed coimmunolocalization experiments for the Slack and Slick subunits with syntaxin, a marker for presynaptic membranes (Fig. 1). Although light microscopy cannot provide definitive information on subcellular localization, Slack and Slick immunoreactivity appears to be present both in the principal cells of MNTB and in the calyces of Held (as visualized by colocalization with syntaxin). No staining was observed with the secondary antibody anti-chicken Alexa Fluor 546, which was used to detect Slack and Slick immunoreactivity (Fig. 1, bottom left). We did, however, detect some nonspecific staining (green) with anti-mouse Alexa Fluor 488, the secondary antibody for the detection of syntaxin (Fig. 1, bottom middle and right), perhaps because of the use of an anti-mouse antibody to stain mouse tissue. Nevertheless, because the anti-mouse secondary antibody did not recognize any morphological structure resembling either the neurons or synaptic terminals in the MNTB, we considered the staining of the calyceal terminals to be specific.

K_{Na} channels from MNTB neurons resemble Slack and Slick channels in expression systems

When expressed in *Xenopus* oocytes, Chinese hamster ovary (CHO) , and human embryonic kidney (HEK) cells, *Slack* and *Slick* give rise to outwardly rectifying potassium channels that have unitary conductances of ~140 and ~180 pS, respectively, in symmetrical potassium solutions (Joiner et al., 1998; Bhattacharjee et al., 2003; Yang et al., 2006). Channels encoded by both genes are gated by increases in intracellular Na^+ concentrations. Although the activity of both channels can be increased by elevating internal Cl^-, this effect is greater for Slick than for Slack (Bhattacharjee et al., 2003). Another particularly important difference between these two channel subunits is that the Slick sub-

unit contains a regulatory nucleotide-binding site that results in activation of this channel in response to a fall in intracellular ATP ($[ATP]_i$) levels (Bhattacharjee et al., 2003).

To examine the biophysical properties of these native K_{Na} channels, inside-out patches were excised from principal neurons of the MNTB. To detect K_{Na} channels, each patch was first exposed to solution containing a high concentration of Na^+ (40–129.5 mM). Channel activity evoked by Na^+ was readily reversible on returning to a Na^+-free medium. Such K_{Na} channel activity was observed in ~30% of >300 patches excised from MNTB neurons.

In 50 initial excised patch experiments, we included the K^+ blockers, 100 nM dendrotoxin and 1 mM tetraethylammonium (TEA), as well as 20 μM ZD-7288 [4-(*N*-ethyl-*N*-phenylamino)-1,2-dimethyl-6-(methylamino)pyridinum chloride] and 1 μM TTX, blockers of H channels and Na^+ channels, respectively, in the bath and in the patch solutions. Slack and Slick channels have been found to be insensitive to dendrotoxin and 1 mM TEA (Joiner et al., 1998; Bhattacharjee et al., 2003), and this mixture of inhibitors permits the isolation of macroscopic K_{Na} currents (see below). We found, however, that the detection of large-conductance Na^+-activated channel activity in patches did not appear to be affected by the presence or absence of these agents. Moreover, the relatively large conductance of K_{Na} channels rendered it straightforward to differentiate them from other channels, and patches containing K_{Na} channels appeared generally devoid of other types of channels. Additional experiments were therefore conducted without the channel blockers.

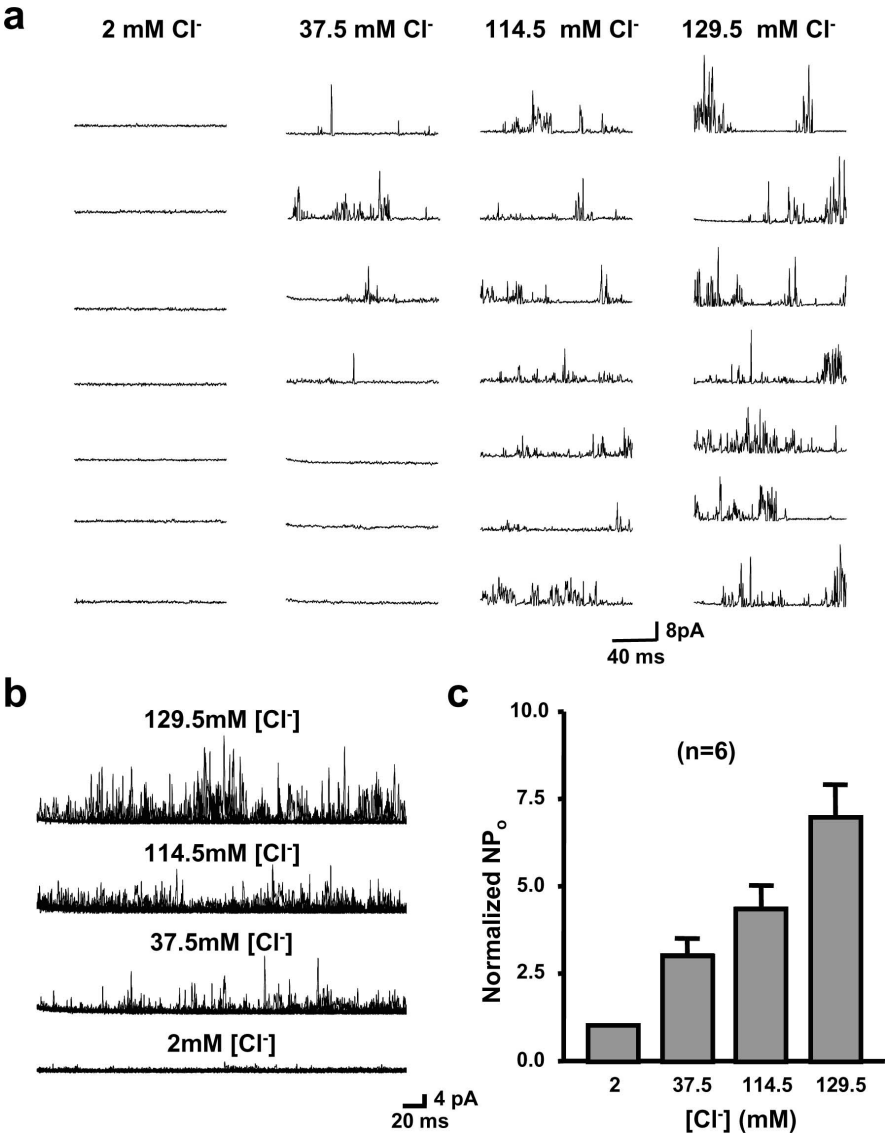

Figure 4. Dependence of MNTB K_{Na} currents on internal chloride concentration. ***a***, Representative traces of channel activity in inside-out patches excised from principal neurons of the MNTB in medium containing 2.0, 37.5, 114.5, or 129.5 mM Cl^- (with 130 mM $[K^+]_i$/2.5 mM $[K^+]_o$, 20 mM $[Na^+]_i$). As in Figure 3, the membrane potential was stepped to 0 mV from a holding potential of −60 mV. ***b***, Twenty superimposed sweeps of channel recordings from inside-out patches placed into solutions containing 2.0, 37.5, 114.5, or 129.5 mM Cl^-. ***c***, Normalized NP_o values determined for different concentrations of Cl^- on the intracellular face of the membrane.

Figure 2*a* illustrates K_{Na} channel activity in an excised patch perfused with a solution containing 10 mM Na^+. We detected large-conductance (>100 pS) outward channel activity in addition to smaller outward conductances (<40 pS) (Fig. 2*a*,*b*, inset). These smaller conductances likely represent subconductance states that have been characterized for both Slack and Slick channels and for native K_{Na} channels in other systems (Dryer, 1994; Joiner et al., 1998; Bhattacharjee et al., 2003), and like the large-conductance state, are dependent on Na^+ (Fig. 3*a*). Patches typically contained multiple K_{Na} channels. To determine the unitary conductance of the major conductance state, six patches were perfused with a low concentration of Na^+ (10 mM) in a modified physiological solution (with 130 mM $[K^+]_i$/2.5 mM $[K^+]_o$ and $[Cl^-]_i$ = 34.5 mM). The voltage was stepped from a holding potential of −60 mV to test potentials of −20, 0, +20, and +40 mV. All point histograms were generated to determine the major unitary current level at these potentials (Fig. 2*b*,*c*). The mean unitary conductance of these MNTB K_{Na} channels (122 ± 4 pS), together with the occurrence of frequent subconductance states, are in close agreement with results found for Slack (~140 pS) and Slick (~180 pS) channels in heterologous expression systems (Joiner et al., 1998; Bhattacharjee et al., 2003), as well as K_{Na} channels in other native cells (Wang et al., 1991; Dryer, 1994; Mistry et al., 1997).

The kinetic behavior of the native MNTB K_{Na} channels (Fig. 2*b*,*c*) was typically intermediate between the rapid flickering activity of Slick channels and the longer "box-like" openings of Slack (Bhattacharjee et al., 2003). The mean burst duration for MNTB channels was 13.0 ± 1.0 ms (n = 10) when recorded with 5 mM Na^+/130 mM Cl^-. Under the same conditions, the mean burst duration for Slick channels expressed in CHO cells was 7.24 ± 1.4 ms, whereas that for Slack was 118 ± 26 ms (Bhattacharjee et al., 2003).

To examine the Na^+ sensitivity of the MNTB channels, the cytoplasmic faces of 10 excised patches containing multiple chan-

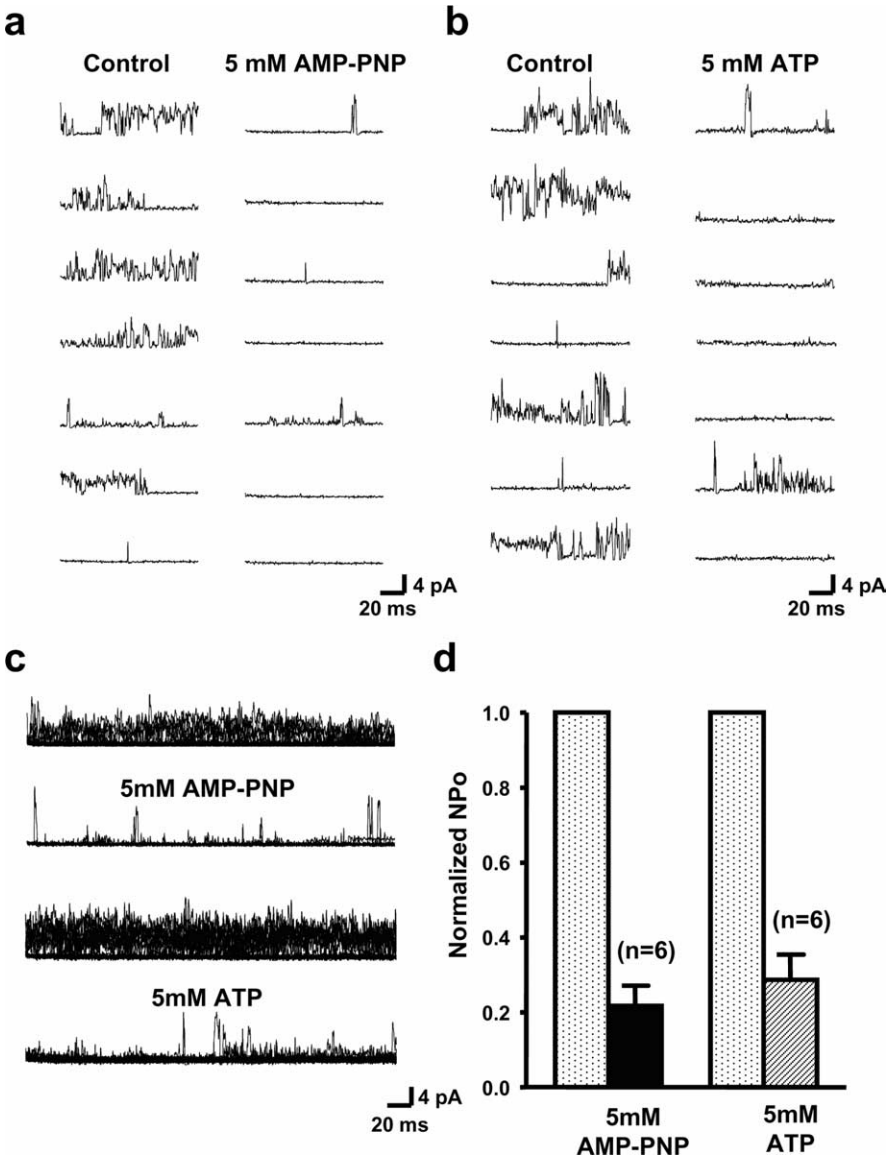

Figure 5. Inhibition of MNTB K_{Na} channels by intracellular ATP. ***a***, Representative traces of channel activity excised from the principal neurons of the MNTB before and after application of the nonhydrolysable ATP analog AMP-PNP (5 mM) to the cytoplasmic face of the patch. The membrane potential was stepped to 0 mV from a holding potential of −60 mV. Ion concentrations were 130 mM $[K^+]_i$/2.5 mM $[K^+]_o$, 20 mM $[Na^+]_i$, and 34.5 mM $[Cl^-]_i$. ***b***, Traces of channel activity from MNTB neurons before and after application of ATP (5 mM; Mg salt) to the cytoplasmic face of the patch. Voltage and ionic conditions are as in ***a***. ***c***, Sixty superimposed sweeps of channel activity before and after application of AMP-PNP or ATP. ***d***, Normalized NP_o values for channel activity recorded before and after application of AMP-PNP or 5 mM ATP to the intracellular face of the patches.

nels were exposed to different concentrations of Na^+ (Fig. 3*a*). Na^+ dependence could be evaluated visually by superimposition of multiple traces at each Na^+ concentration (Fig. 3*b*) and was quantified by calculation of NP_o (number of channels times probability of opening). The effects of changing concentrations of Na^+ were readily reversible (Fig. 3*c*). To combine results from separate patches containing different numbers of channels, these data were normalized to values of NP_o measured at 80 mM Na^+. The combined data provides a calculated EC_{50} of 77 mM and a Hill coefficient of 1.46 for gating of the native K_{Na} channels by Na^+ (Fig. 3*d*). This is consistent with previously reported EC_{50} values of 41 and 89 mM and Hill coefficients of 1.4 and 2.4 for Slack and Slick channels, respectively (Joiner et al., 1998; Bhattacharjee et al., 2003). Because there is no channel activity with 0 mM Na^+, the MNTB channels resemble Slack rather than Slick channels, which, in expression systems, can readily be detected even in the absence of Na^+ (Bhattacharjee et al., 2003).

We also tested the effects of changing Cl^- concentrations at the cytoplasmic face of the channels (Fig. 4*a*,*b*). To combine the results from six multichannel patches in which we tested the effects of altered Cl^- concentrations, we normalized the NP_o values for each patch to those measured at 2 mM Cl^-. We found an ~6.9-fold increase in activity on changing Cl^- from 2 to 129.5 mM (Fig. 4*c*). Previous data have shown that both Slack and Slick channels can be activated by internal Cl^-, although this effect is greater for Slick than for Slack (Bhattacharjee et al., 2003). The Cl^- sensitivity of the MNTB K_{Na} channels more closely resembles that of Slick (fivefold increase in channel activity when cytoplasmic Cl^- is raised from 3 to 130 mM) rather than that of Slack (only a twofold increase under the same conditions).

The *Slick* channel subunit has a binding site for ATP at its C terminus. The binding of ATP to this site produces a significant reduction in channel activity (Bhattacharjee et al., 2003). This site is absent from the *Slack* channel. We therefore tested the effects of ATP and of AMP-PNP (5′-adenylyl-imidodiphosphate), a nonhydrolyzable ATP analog, on MNTB K_{Na} activity (Fig. 5). In six patches, exposure of the cytoplasmic face to AMP-PNP (5 mM) produced an ~70–80% reduction in channel activity (Fig. 5*a*,*c*,*d*). Exposure of excised patches to ATP itself (5 mM) also produced a quantitatively similar reduction in activity (Fig. 5*b*,*c*,*d*). These findings suggest that Slick subunits are likely to contribute to the native K_{Na} channel activity.

In summary, channel recordings from the principal neurons of the MNTB revealed native K_{Na} channels with properties resembling those of Slack and Slick channels in transfected cells. Because both Slack and Slick are expressed in these neurons, the native K_{Na} channels may represent heteromultimers of these two subunits.

K_{Na} currents are a major component of whole-cell K^+ current in MNTB neurons

To examine whole-cell macroscopic K_{Na} currents in MNTB neurons, we performed whole-cell recordings in the presence of pharmacological agents known to block other known components of current in these cells. In particular, brainstem slices were superfused with extracellular medium containing 1 μM TTX, 20 μM ZD-7288, 100 nM dendrotoxin, and 1 mM TEA to block the Na^+ current, the I_h current (hyperpolarization-activated cation current) (BoSmith et al., 1993; Harris and Constanti, 1995), and the Kv1 family and Kv3 family of potassium currents known to be present in these neurons (Manis and Marx, 1991; Brew and For-

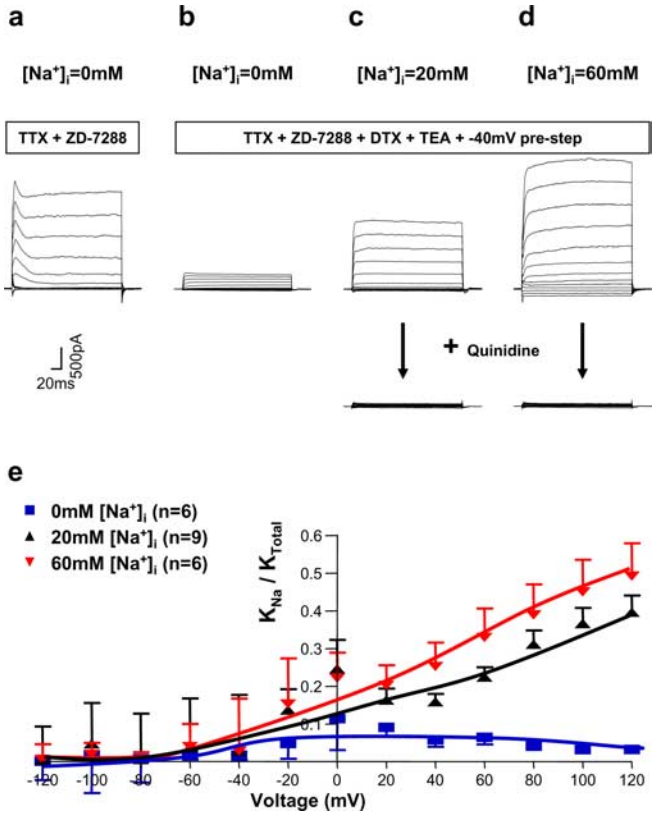

Figure 6. Macroscopic MNTB K_{Na} currents are activated by $[Na^+]_i$. ***a***, Whole-cell K_{Na} currents recorded from a principal neuron of the MNTB in the presence of 1 μM TTX and 20 μM ZD-7288 to block Na^+ and I_h currents and with no Na^+ in the intracellular patch solution. Steps were given from a holding potential of −70 mV to test potentials between −120 and +120 mV in 20 mV increments. ***b–d***, Whole-cell K_{Na} currents recorded from the principal neurons of the MNTB using the same voltage protocol as in ***a*** in the presence of 1 μM TTX, 20 μM ZD-7288, together with 100 nM dendrotoxin (DTX) and 1 mM TEA in the ACSF to block Kv1 family and Kv3 family of potassium currents known to be present in these neurons. A 600 ms prepulse to −40 mV before voltage steps to test potentials was also applied to eliminate a small and rapidly inactivating component of K^+ current. Traces in ***b–d*** were recorded with patch pipettes containing 0, 20, and 60 mM Na^+, respectively. The bottom panels of ***c*** and ***d*** show that bath application of 1 mM quinidine eliminated these native K_{Na} currents. ***e***, Summary data showing the amplitude of the macroscopic K_{Na} currents with 0, 20, and 60 mM Na^+ in the recording pipettes.

sythe, 1995; Wang et al., 1998). Neither of the two K^+ channel blockers affects either Slack or Slick currents at these concentrations (Bhattacharjee et al., 2003). In addition, we applied a 600 ms prepulse to −40 mV before voltage steps to test potentials. This prepulse eliminated a small and rapidly inactivating component of K^+ current that may represent Kv4 family channels (Dever et al., 2004). Under these conditions, the amplitude of the remaining whole-cell K^+ current was highly sensitive to the level of Na^+ in the patch pipette (Fig. 6). The activation of these native K_{Na} currents occurs relatively rapidly (<20 ms) after a step depolarization. In this respect, the currents more closely resemble rapidly activating currents observed in *Slick*-transfected cells, rather than the slowly activating currents of *Slack*-expressing cells (Bhattacharjee et al., 2003). To determine the proportion of total MNTB neuron K^+ current that can be attributed to K_{Na} channels, we first recorded whole-cell currents in the presence of only 1 μM TTX and 20 μM ZD-7288. We then applied the K^+ channel blockers dendrotoxin (100 nM) and TEA (1 mM) and again recorded the remaining current. Figure 6*e* plots the proportion of remaining K^+ current at different test potentials for cells dialyzed with 0, 20, or 60 mM internal Na^+. Under the latter two conditions, K_{Na} current constituted 40–60% of the total K^+ current. The increases in macroscopic currents with 20 or 60 mM internal Na^+ were statistically significant ($p < 0.0004$ for 20 mM Na^+ and $p < 0.0002$ for 60 mM Na^+ at +80 to +120 mV).

Previous studies have identified quinidine as a potent inhibitor of both Slack and Slick currents (Bhattacharjee et al., 2003; Yang et al., 2006). Bath application of 1 mM quinidine greatly inhibited the Na^+-sensitive component of whole-cell K^+ current in MNTB neurons (Fig. 6*c*,*d*, bottom panels). In addition, our previous data have identified bithionol [2,2′-thiobis(4,6-dichlorophenol)], a bis-phenol anti-parasitic compound (Enzie and Colglazier, 1960; Barr et al., 1965), to be an effective opener of Slack channels (Yang et al., 2006). Exposure of *Slack*-transfected HEK cells to 10 μM bithionol produces an increase in whole-cell Slack current that decreases toward control level after washout of bithionol (Yang et al., 2006). In the present study, we found that as in *Slack*-transfected cells, perfusion of bithionol onto the slices increased native K_{Na} currents by values of 32.7 ± 9.5, 34. 0 ± 60.6, 40.0 ± 9.3, 45.7 ± 1 1.2, and 48.1 ± 1 2.6% elicited by voltage steps of 40, 60, 80, 100, and 120 mV, respectively ($n = 5$) (Fig. 7*a–c*). These pharmacological findings with both quinidine and bithionol strongly suggest that the Slack and Slick subunits contribute to the K_{Na} current of MNTB neurons.

K_{Na} channels regulate the accuracy of timing of MNTB neurons

In the presence of cytoplasmic Na^+, Slack and Slick K_{Na} channels open near the resting potential of the cells (approximately −60 mV). It is known that, for brainstem auditory neurons, an increase in membrane conductance near the resting potential significantly increases the accuracy of timing of action potentials (Manis and Marx, 1991). Indeed, Kv1.1 and Kv1.2 channels that are located in the axons of MNTB neurons and also activate near rest are known to reduce jitter in the timing of evoked action potentials (Brew et al., 2003; Kopp-Scheinpflug et al., 2003). An increase in resting membrane conductance produces a decrease in the membrane time constant, allowing stimuli to trigger action potentials that are more closely linked to the onset of the stimulus. To determine whether the level of resting K_{Na} current influences the accuracy of timing of MNTB neurons, we recorded their responses to 100 ms trains of intracellular current pulses (0.3 ms, 2 nA) applied at frequencies of 10–400 Hz, using patch pipettes containing different levels of Na^+ (0, 5, 20, and 40 mM).

The general way that the firing pattern of MNTB neurons responds to increases in stimulation frequency was the same for all levels of intracellular Na^+ and is illustrated in Figure 8 for an MNTB neuron dialyzed with 20 mM $[Na^+]_i$. At all stimulus frequencies up to 170 Hz, this neuron responded to each stimulus pulse with an action potential ("regular" firing). At higher stimulus frequencies, it continued to respond but not all stimulus pulses evoked action potentials (Fig. 8, middle traces). At frequencies of stimulation (~180–230 Hz) that are just slightly higher than those at which the neuron is capable of generating an action potential in response to every stimulus (<170 Hz), the timing of evoked action potentials is scattered with respect to the stimulus pulses ("irregular" firing). Interestingly, as the stimulus frequency was raised still further, the strict phase locking of action potentials to the stimulus pulse was restored when the neuron fired a single action potential in response to every other stimulus pulse (Fig. 8, right traces, 240–300 Hz). When the stimulus frequency increased past 240 Hz, this cell responded to high-frequency stimulation with a lower frequency of firing that re-

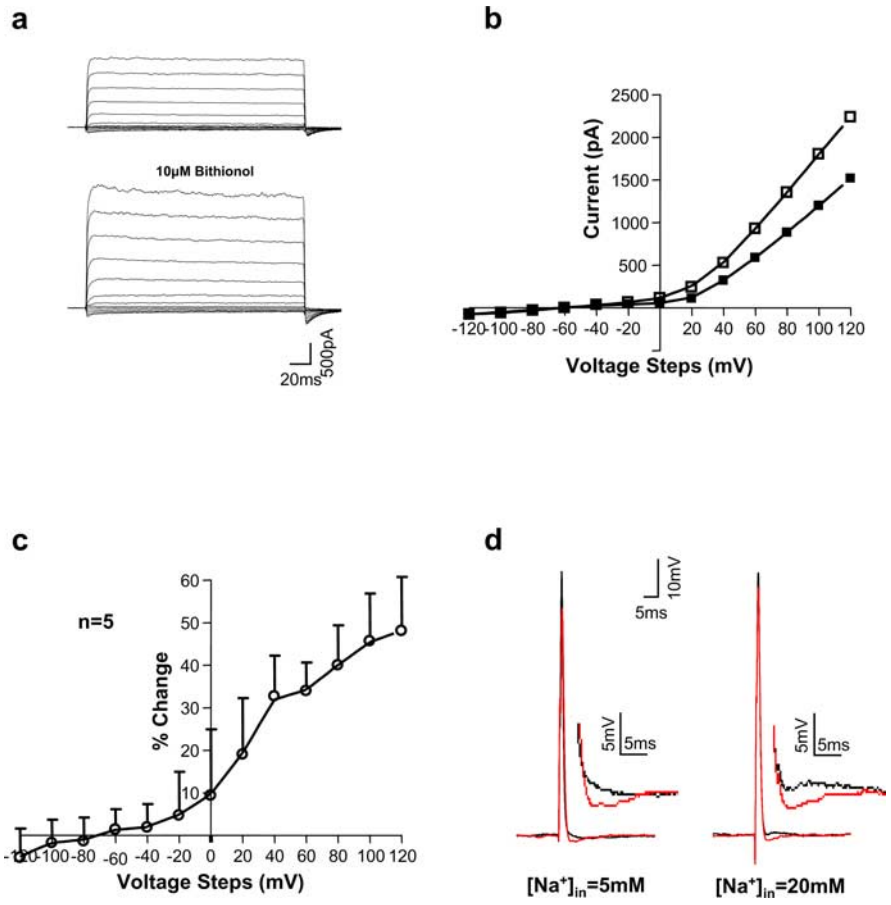

Figure 7. Bithionol enhances native K_{Na} currents and the AHPs of MNTB neurons. ***a***, Representative whole-cell K_{Na} current recordings from a principal neuron of the MNTB with ACSF containing 1 μM TTX, 100 nM dendrotoxin, 1 mM TEA, and 20 μM ZD-7288 and a 600 ms prestep of −40 mV with 20 mM $[Na^+]_i$ before and after bath application of 10 μM bithionol. ***b***, *I–V* curves of whole-cell K_{Na} currents in MNTB neurons before (filled squares) and after (open squares) 10 μM bithionol. ***c***, Summary data showing percentage of change of native K_{Na} currents in MNTB neurons at different voltages after exposure to 10 μM bithionol. ***d***, Bithionol enhances the AHP that follows MNTB neuron action potentials evoked by a single depolarizing current pulse. Superimposed traces show action potentials before (black) and after (red) 10 μM bithionol. The insets show AHPs at higher magnification.

mains phase locked to individual stimulus pulses, a property previously reported for MNTB neurons and other auditory neurons (Brownell, 1975; Banks and Smith, 1992; Wu and Kelly, 1993).

To evaluate the temporal fidelity of the action potentials evoked by different stimulus frequencies and different levels of intracellular Na^+, we calculated the strength of the phase vector that relates the timing of evoked action potentials to the onset of the stimulus pulses during the 100 ms stimulus trains (see Materials and Methods). Perfect phase locking is associated with a phase vector strength of one. When phase vector strength is plotted as a function of stimulus frequency, dips in the value of the vector strength are observed for frequencies at which action potentials are not perfectly locked to the stimuli. Figure 9*a* shows the vector strength plot for the cell shown in Figure 8. Although vector strength declines with increasing frequency for all levels of intracellular Na^+, the "dips" in vector strength that occur when stimuli fail to evoke action potentials at a regular frequency were reduced significantly with increasing $[Na^+]_i$, as is shown in Figure 9*b*, which compares the mean vector strength in cells dialyzed with 0, 5, 20, or 40 mM Na^+. The differences in vector strength at 200 and 400 Hz for cells with 0 or 40 mM Na^+ were statistically significant (0.90 ± 0.01 vs 0.98 ± 0.004, $p < 0.0001$ at 200 Hz; 0.75 ± 0.02 vs 0.85 ± 0.03, $p < 0.03$ at 400 Hz).

Computer simulations predict that K_{Na} channels improve fidelity of timing

To determine whether the effect of increases in $[Na^+]_i$ on the timing of evoked action potentials is consistent with enhanced K_{Na} current, we performed numerical simulations of MNTB neurons. We used a previously developed computer model of MNTB neurons that incorporates a voltage-dependent Na^+ current, a leakage current, and low-threshold (Kv1 family) and high-threshold (Kv3 family) voltage-dependent potassium currents (Perney and Kaczmarek, 1997; Wang et al., 1998; Song et al., 2005). To this model, we added a K_{Na} current with properties intermediate between those of Slack and Slick (Bhattacharjee et al., 2003, 2005) (see Materials and Methods). We maintained intracellular Na^+ levels in the model fixed at 0, 5, 20, or 40 mM and adjusted E_{Na} accordingly. In qualitative agreement with recordings of real MNTB neurons, we found that elevation of Na^+ levels in the model improved the timing of action potentials at stimulus frequencies above those at which the neurons are capable of firing an action potential in response to every stimulus pulse. As in MNTB neurons, the phase-vector strength declines with increasing frequency for all levels of intracellular Na^+, but the dips in vector strength that occur when stimuli fail to evoke action potentials at a regular frequency are substantially reduced with high $[Na^+]_i$ (Fig. 9*c*,*d*).

The Slack channel activator bithionol increases temporal fidelity of MNTB neurons

As described above, exposure of MNTB neurons to bithionol increases the amplitude of native K_{Na} current. Use of this agonist allows one to determine the effects of a change in K_{Na} current without altering the driving force for Na^+ entry (a change from 5 to 20 or 40 mM intracellular Na^+ would be expected to change E_{Na} from +50 to +45 or +28 mV, respectively). Exposure to bithionol enhanced the afterhyperpolarization (AHP) that follows an action potential evoked by a single brief depolarizing current pulse or produced an AHP in cases in which none was evident before bithionol exposure (Fig. 7*d*). The amplitude of this AHP was enhanced by bithionol [from 0.67 ± 0.09 to 1.61 ± 0.10 mV, when $[Na^+]_{in} = 5$ mM ($n = 6$, $p < 0.01$); from 0.53 ± 0.04 to 1.95 ± 0.17 mV, when $[Na^+]_{in} = 20$ mM ($n = 6$, $p < 0.01$)]. In contrast, the duration of the AHP was not affected by bithionol [16.06 ± 0.86 vs 16.98 ± 0.53 ms, when $[Na^+]_{in} = 5$ mM ($n = 6$); 15.9 ± 0.73 vs 15.99 ± 1.14 ms, when $[Na^+]_{in} = 20$ mM ($n = 6$)]. Furthermore, in cells perfused with a fixed level of intracellular Na^+ (20 mM), the fidelity of timing of action potentials evoked by a 100 ms train of intracellular current pulses applied at frequencies greater than ~150 Hz was reversibly enhanced by exposure of the MNTB neurons to bithionol (as shown by one example in Fig. 9*e*). As with elevations of intracellular Na^+, bithionol increased the value of the phase vector strength ($n = 5$ cells) at those

frequencies at which stimulation fails to evoke action potentials at a strictly regular frequency (Fig. 9*f*). The difference in vector strength at 200 Hz for recordings before and during 10 μM bithionol application was statistically significant (0.89 ± 0.02 vs 0.95 ± 0.02; $p < 0.05$).

Discussion

Slack (Slo2.2) and Slick (Slo2.1) are ligand-gated K^+ channels activated by intracellular Na^+ and Cl^- ions and are abundantly expressed in the CNS of mammals (Joiner et al., 1998; Bhattacharjee et al., 2002). In this study, we found that both channel subunits are expressed at high levels in presynaptic and postsynaptic elements of the MNTB. Using whole-cell and excised patch recordings, as well as pharmacological approaches, we have demonstrated that in addition to the voltage-dependent potassium channels that have been extensively characterized in these neurons (Manis and Marx, 1991; Brew and Forsythe, 1995; Wang et al., 1998; Song et al., 2005), these neurons also have a major component of K^+ current that is sensitive to cytoplasmic levels of Na^+ and Cl^-, and the properties of the channels that underlie this current closely resemble those of Slack and Slick channels. Furthermore, by manipulating intracellular levels of Na^+ and by using the *Slack* activator bithionol, we found that the accuracy of timing of action potentials in MNTB neurons during high-frequency stimulation is sensitive to the level of this K_{Na} current, a result that is also consistent with computer simulations of MNTB neurons.

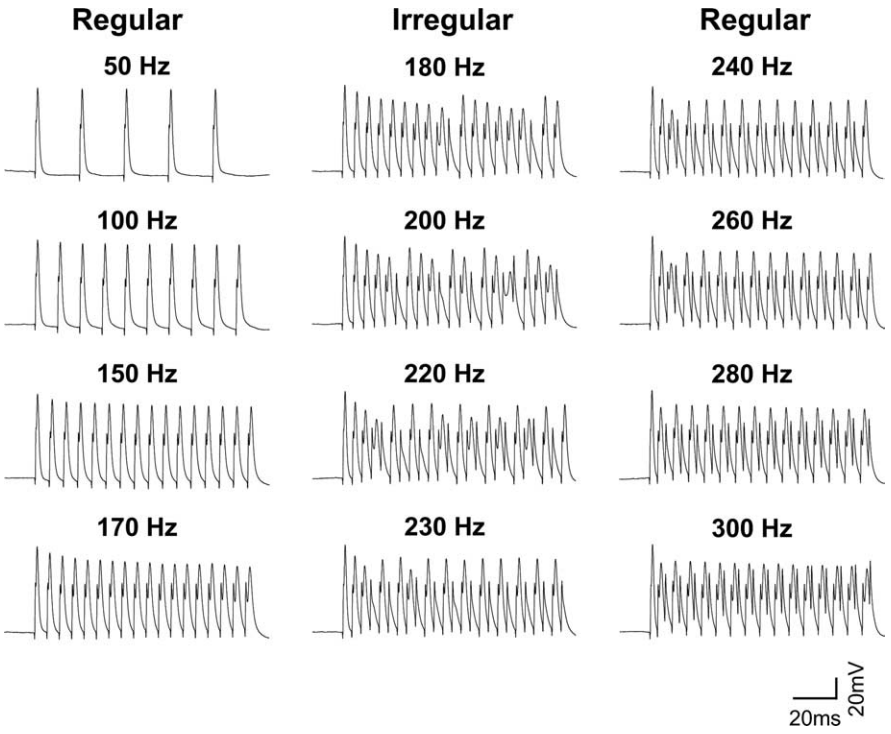

Figure 8. Response to MNTB neurons to increasing rates of stimulation. Action potential responses of an MNTB neuron recorded with a patch pipette containing 20 mM Na^+. The neuron was stimulated with a train of depolarizing current pulses applied at frequencies from 50 to 300 Hz. At stimulus frequencies up to 170 Hz, action potentials were evoked by every stimulus pulse (left traces). At 180–230 Hz, the timing of evoked action potentials became scattered with respect to the stimulus pulses (middle traces). When the stimulus frequency was increased past 240 Hz, this cell responded to high-frequency stimulation with a lower frequency of firing that remains locked to individual stimuli (right traces).

The properties of the channels that are activated by elevations of Na^+ at the cytoplasmic face of excised patches from MNTB neurons are intermediate between those of Slack and Slick and may represent either heteromers of these two subunits (Chen et al., 2006) or may reflect association of these subunits with as yet uncharacterized ancillary subunits. Their large unitary conductance differentiates them from most other types of K^+ channels. Only large-conductance Ca^{2+}-activated K^+ channels (maxi-K channels) have a comparably large conductance. Our laboratory and that of others (I. D. Forsythe, personal communication) have, however, found that little or no maxi-K type Ca^{2+}-activated K^+ current can be recorded at the soma of MNTB neurons. Moreover, maxi-K channels are not activated by Na^+ or Cl^- ions and are potently blocked by 1 mM TEA, whereas the K_{Na} channels in MNTB neurons could readily be recorded in the presence of this agent.

In transfected cells, the macroscopic characteristics of Slack and Slick subunits are quite different from each other (Bhattacharjee et al., 2003). Slick activation occurs very rapidly with step changes in voltage, whereas Slack currents increase only slowly after a step depolarization. Three pieces of evidence suggest that the Slick subunit is likely to play a dominant role in the characteristics of the MNTB K_{Na} current. First, the relatively rapid activation of the native K_{Na} current (<20 ms) (Figs. 6, 7) in response to depolarizing commands more closely resembles that of Slick than Slack. Second, Slick channels are more sensitive to changes in intracellular Cl^- than are Slack channels. The degree of sensitivity of the native current to intracellular chloride (an ~6.9-fold increase in activity on changing Cl^- from 2 to 129.5 mM) more closely matches that found for Slick (Bhattacharjee et al., 2003). Finally, the fact that the native channel activity can be decreased by a nonhydrolyzable ATP analog strongly suggests that Slick, which is regulated by a consensus ATP-binding site in its C terminus (Bhattacharjee et al., 2003), is likely to be a component of the native channel. Nevertheless, the kinetic behavior of the channels cannot be used alone to differentiate Slack from Slick channels, because recent work has shown that an alternative isoform of Slack, termed Slack-A, activates rapidly in response to depolarizations (Bhattacharjee et al., 2004).

We also found that the accuracy of timing of MNTB neurons is increased under conditions in which K_{Na} channels are activated. This effect was observed both with elevations of intracellular Na^+ by dialysis through patch pipettes and by exposure to the *Slack* activator bithionol. Previous work has revealed that, at fixed Na^+ concentrations, bithionol produces a significant increase in mean *Slack* channel open probability, apparently by decreasing channel closed times (Yang et al., 2006). As with some other channel agonists, the mechanism of bithionol action may involve an allosteric interaction with regions of the channel that control gating. Those data represent, to the best of our knowledge, the first demonstration of activation of Slack currents (or K_{Na}) by any compound. Although we cannot be certain that bithionol does not also have uncharacterized targets other than K_{Na} channels in MNTB neurons, the observed effects of this agent both on ionic currents and on firing characteristics are consistent with selective enhancement of K_{Na} current. In expression sys-

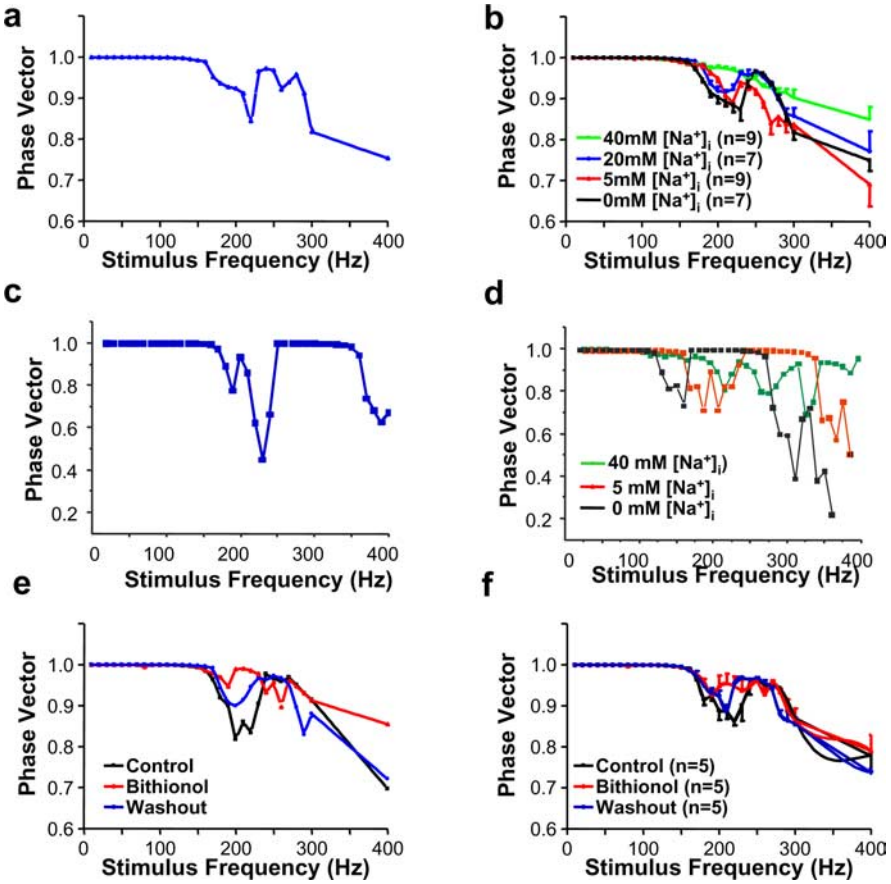

Figure 9. K_{Na} channels regulate the accuracy of timing of MNTB neurons. ***a***, Plot of phase vector strength as a function of stimulus frequency for the cell shown in Figure 8. ***b***, Summary of phase vector-strength experiments with 0, 5, 20, or 40 mM $[Na^+]_i$. ***c***, A plot of phase vector strength as a function of stimulus frequency for numerical simulations of a model MNTB neuron with a K_{Na} current with properties intermediate between those of *Slack* and *Slick* and with 20 mM $[Na^+]_i$. ***d***, Superimposed plots of phase vector strength as a function of stimulus frequency for the model neuron with 0, 5, and 40 mM $[Na^+]_i$. The vector strength declines with increasing frequency for all levels of intracellular Na^+, but the dips in vector strength that occur when stimuli fail to evoke action potentials at a regular frequency are substantially reduced with increasing $[Na^+]_i$. ***e***, Plot of phase vector strength as a function of stimulus frequency for a real MNTB neuron with 20 mM $[Na^+]_i$ before and after perfusion of 10 μM bithionol onto the slice and after washout of bithionol. ***f***, Summary of phase vector strength experiments in cells before and after perfusion with 10 μM bithionol.

tems, biothionol has also been found to activate maxi-K Ca^{2+}-activated K^+ channels (V. Gribkoff, personal communication). As described above, however, there appears to be little or no Ca^{2+}-activated K^+ current at the somata of MNTB neurons. The effect of increased K_{Na} current on the timing of action potentials is therefore likely to influence the fidelity of information transmission through MNTB under conditions of rapid firing, when cytoplasmic Na^+ levels are elevated.

The time course and the extent of elevations on intracellular Na^+ at the somata of MNTB neurons during high-frequency firing have yet to be determined. In unstimulated muscle cells, basal Na^+ concentrations have been estimated to be between ~4 and 15 mM (Lee and Fozzard, 1975; Ellis, 1977; Kameyama et al., 1984; Nakaya et al., 1990). During high-frequency stimulation of neurons, however, $[Na^+]_i$ reaches a concentration of 45–100 mM in certain locations (Rose, 2002). The two major pathways for Na^+ entry during neuronal activity are through voltage-dependent Na^+ channels and through ionotropic ligand-gated receptors, such as AMPA and NMDA glutamate receptors. Elevation of intracellular Na^+ by these pathways produces highly localized elevations in Na^+ (Rose and Ransom, 1997; Rose and Konnerth, 2001; Zhong et al., 2001). Moreover, recovery to baseline Na^+ levels is often very slow and, in many cases, requires tens of seconds (Rose, 2002).

It is not yet known whether Slack or Slick subunits in neurons are physically associated with voltage-dependent Na^+ channels. Such close proximity could result in substantially higher local levels of $[Na^+]_i$ near K_{Na} channels than in bulk cytoplasm (Dryer, 1994). In peripheral axons of *Xenopus* neurons, a close correlation has been found between the localization of K_{Na} channels and voltage-dependent Na^+ channels, suggesting the two channel types are targeted to the same membrane locations (Koh et al., 1994). Although studies of the role of K_{Na} channels in neurons have focused on their activation by Na^+ influx through voltage-dependent channels, large elevations of $[Na^+]_i$ also occur as a result after activation of Na^+-permeable receptors such as glutamate receptors. The Slack subunit has been shown to bind directly to the PDZ domain of PSD-95, a major component of glutamatergic postsynaptic densities (Uchino et al., 2003). Direct activation of Na^+ influx through glutamate receptors using kainate has been proposed to activate K_{Na} channels (Liu et al., 1998).

All of the recordings in the present study were conducted at RT (21–22°C), a common practice in *in vitro* studies because it favors tissue survival and improves voltage-clamp conductances with rapid kinetics. Higher temperatures have been shown to allow higher-frequency and more prolonged transmission at the calyx of Held (Taschenberger and von Gersdorff, 2000; Kushmerick et al., 2006) and other excitatory synapses (Saviane and Silver, 2006), and recent work has suggested that a primary contribution to postsynaptic temperature sensitivity is an alteration in AMPA receptor kinetics (Postlethwaite et al., 2006). Although the kinetics of the K_{Na} currents and that of other channels are likely to be more rapid at higher temperatures (Cao and Oertel, 2005), several considerations suggest that the qualitative effect of K_{Na} channels on the timing and firing patterns of MNTB neurons are likely to persist at *in vivo* temperatures. First, the mean conductance of many channels that, like K_{Na} channels, possess multiple conductance states has been found to increase at higher temperatures (Colquhoun and Sakmann, 1985; Fox, 1987; Dilger et al., 1991), suggesting that the contribution of K_{Na} currents may increase at elevated temperatures. Second, our numerical simulations have indicated that the increase in temporal accuracy after an increase in K_{Na} current results primarily from the shortening of the membrane time constant and decrease in input resistance, which decrease the threshold for action potential generation and also result in evoked action potentials being linked closely in time to the onset of depolarizing stimuli. Because these basic effects persist over a wide range of model parameters (data not shown), and are evident in completely generic neuronal sim-

ulations (Bhattacharjee et al., 2003), they are unlikely to be highly sensitive to temperature. In many respects, this proposed role for K_{Na} channels resembles that of "low-threshold" Kv1.1 and Kv1.2 channels, which are located in axons of many auditory neurons where they control input resistance and action potential timing both in brain slices at RT and *in vivo* at physiological temperatures (Manis and Marx, 1991; Brew and Forsythe, 1995; Wang et al., 1998; Brew et al., 2003; Kopp-Scheinpflug et al., 2003). K_{Na} channels, however, differ from these voltage-dependent K^+ channels in that they are located at the somata, and their activity becomes enhanced only after Na^+ entry.

In summary, our results indicate that Na^+-activated K^+ channels with properties resembling those of Slack and Slick channels in transfected cells are present in MNTB neurons. Moreover, our findings suggest that the native K_{Na} channels may play an important role in adapting the pattern of firing to different rates of stimulation and influence the fidelity of information through the MNTB.

References

Banks M, Smith PH (1992) Intracellular recordings from neurobiotin-labeled cells in brain slices of the rat medial nucleus of the trapezoid body. J Neurosci 12:2819–2837.

Barnes-Davies M, Forsythe ID (1995) Pre- and postsynaptic glutamate receptors at a giant excitatory synapse in rat auditory brainstem slices. J Physiol (Lond) 488:387–406.

Barr FS, Collins GF, Wyatt LG (1965) Potentiation of the antimicrobial activity of bithionol. J Pharm Sci 54:801–802.

Bhattacharjee A, Gan L, Kaczmarek LK (2002) Localization of the Slack potassium channel in the rat central nervous system. J Comp Neurol 454:241–254.

Bhattacharjee A, Joiner WJ, Wu M, Yang Y, Sigworth FJ, Kaczmarek LK (2003) *Slick* (*Slo*2.1), a rapidly-gating sodium-activated potassium channel inhibited by ATP. J Neurosci 23:11681–11691.

Bhattacharjee A, von Hehn CAA, Kaczmarek LK (2004) An alternative transcript of the sodium-activated potassium channel Slack exhibits fast gating kinetics. Soc Neurosci Abstr 30:635.15.

Bhattacharjee A, von Hehn CA, Mei X, Kaczmarek LK (2005) Localization of the Na^+-activated K^+ channel Slick in the rat central nervous system. J Comp Neurol 484:80–92.

BoSmith RE, Briggs I, Sturgess NC (1993) Inhibitory actions of ZENECA ZD7288 on whole-cell hyperpolarization activated inward current (If) in guinea-pig dissociated sinoatrial node cells. Br J Pharmacol 110:343–349.

Brew HM, Forsythe ID (1995) Two voltage-dependent K^+ conductances with complementary functions in postsynaptic integration at a central auditory synapse. J Neurosci 15:8011–8022.

Brew HM, Hallows JL, Tempel BL (2003) Hyperexcitability and reduced low threshold potassium currents in auditory neurons of mice lacking the channel subunit Kv1.1. J Physiol (Lond) 548:1–20.

Brownell WE (1975) Organization of the cat trapezoid body and the discharge characteristics of its fibers. Brain Res 94:413–433.

Cao XJ, Oertel D (2005) Temperature affects voltage-sensitive conductances differentially in octopus cells of the mammalian cochlear nucleus. J. Neurophysiol 94:821–832.

Chen H, Yang Y, Gazula V, Yan Y, Sigworth F, Kaczmarek LK (2006) Slick and Slack form heteromeric sodium-activated potassium channels in neurons. Biophys J 90:1559a.

Colquhoun D, Sakmann B (1985) Fast events in single-channel currents activated by acetylcholine and its analogues at the frog muscle end-plate. J Physiol (Lond) 369:501–557.

Dever D, Casseday JH, Covey E (2004) Differential expression of Kv4.2 and 4.3 ion channel subunits in the auditory brainstem and midbrain of the big brown bat *Eptesicus fuscus*. Soc Neurosci Abstr 30:304.2.

Dilger JP, Brett RS, Poppers DM, Liu Y (1991) The temperature dependence of some kinetic and conductance properties of acetylcholine receptor channels. Biochim Biophys Acta 1063:253–258.

Dryer SE (1994) Na^+-activated K^+ channels: a new family of large-conductance ion channels. Trends Neurosci 17:155–160.

Egan TM, Dagan D, Kupper J, Levitan IB (1992) Na^+-activated K^+ channels are widely distributed in rat CNS and in *Xenopus* oocytes. Brain Res 584:319–321.

Ellis D (1977) The effects of external cations and ouabain on the intracellular sodium activity of sheep heart Purkinje fibres. J Physiol (Lond) 273:211–240.

Enzie FD, Colglazier ML (1960) Preliminary trials with bithionol against tapeworm infections in cats, dogs, sheep, and chickens. Am J Vet Res 21:628–630.

Forsythe ID, Barnes-Davies M (1993) The binaural auditory pathway: excitatory amino acid receptors mediate dual timecourse excitatory postsynaptic currents in the rat medial nucleus of the trapezoid body. Proc Biol Sci 251:151–157.

Fox JA (1987) Ion channel subconductance states. J Membr Biol 97:1–8.

Hamill OP, Marty A, Neher E, Sakmann B, Sigworth FJ (1981) Improved patch-clamp techniques for high-resolution current recording from cells and cell-free membrane patches. Pflügers Arch 391:85–100.

Harris NC, Constanti A (1995) Mechanism of block by ZD 7288 of the hyperpolarization-activated inward rectifying current in guinea pig substantia nigra neurons in vitro. J Neurophysiol 74:2366–2378.

Hille B (2001) Ionic channels of excitable membranes. Sunderland, MA: Sinauer.

Isaacson JS, Walmsley B (1995) Receptors underlying excitatory synaptic transmission in slices of the rat anteroventral cochlear nucleus. J Neurophysiol 73:964–973.

Joiner WJ, Tang MD, Wang L-Y, Dworetzky SI, Boissard CG, Gan L, Gribkoff VK, Kaczmarek LK (1998) Formation of intermediate-conductance calcium-activated potassium channels by interaction of Slack and Slo subunits. Nat Neurosci 1:462–469.

Kameyama M, Kakei M, Sato R, Shibasaki T, Matsuda H, Irisawa H (1984) Intracellular Na^+ activates a K^+ channel in mammalian cardiac cells. Nature 309:354–356.

Koh DS, Jonas P, Vogel W (1994) Na^+-activated K^+ channels localized in the nodal region of myelinated axons of *Xenopus*. J Physiol (Lond) 479:183–197.

Kopp-Scheinpflug C, Fuchs K, Lippe WR, Tempel BL, Rubsamen R (2003) Decreased temporal precision of auditory signaling in Kcna1-null mice: an electrophysiological study *in vivo*. J Neurosci 23:9199–9207.

Kushmerick C, Renden R, von Gersdorff H (2006) Physiological temperatures reduce the rate of vesicle pool depletion and short-term depression via an acceleration of vesicle recruitment. J Neurosci 26:1366–1377.

Lee CO, Fozzard HA (1975) Activities of potassium and sodium ions in rabbit heart muscle. J Gen Physiol 65:695–708.

Lenn NJ, Reese TS (1966) The fine structure of nerve endings in the nucleus of the trapezoid body and the ventral cochlear nucleus. Am J Anat 118:375–389.

Levitan IB, Kaczmarek LK (2002) The neuron: cell and molecular biology. New York: Oxford UP.

Liu QY, Schaffner AE, Barker JL (1998) Kainate induces an intracellular Na^+-activated K^+ current in cultured embryonic rat hippocampal neurons. J Physiol (Lond) 510:721–734.

Liu SQ, Kaczmarek LK (1998) Depolarization selectively increases the expression of the Kv3.1 potassium channel in developing inferior colliculus neurons. J Neurosci 18:8758–8769.

Macica CM, von Hehn CA, Wang L-Y, Ho CS, Yokoyama S, Joho RH, Kaczmarek LK (2003) Modulation of the Kv3.1b potassium channel isoform adjusts the fidelity of the firing pattern of auditory neurons. J Neurosci 23:1133–1141.

Magistretti J, Mantegazza M, Guatteo E,. Wanke E (1996) Action potentials recorded with patch-clamp amplifiers: are they genuine? Trends Neurosci 19:530–534.

Manis PB, Marx SO (1991) Outward currents in isolated ventral cochlear nucleus neurons. J Neurosci 11:2865–2880.

Mistry DK, Tripathi O, Chapman RA (1997) Kinetic properties of unitary Na^+-dependent K^+ channels in inside-out patches from isolated guinea-pig ventricular myocytes. J Physiol (Lond) 500:39–50.

Morest DK (1968) The collateral system of the medial nucleus of the trapezoid body of the cat, its neuronal architecture and relation to the olivocochlear bundle. Brain Res 9:288–311.

Morest DK (1973) Auditory neurons of the brain stem. Adv Otorhinolaryngol 20:337–356.

Nakaya H, Hattori Y, Tohse N, Shida S, Kanno M (1990) Beta-adrenoceptor-mediated depolarization of the resting membrane in

guinea-pig papillary muscles: changes in intracellular Na^+, K^+ and Cl^- activities. Pflügers Arch 417:185–193.

Perney TM, Kaczmarek LK (1997) Localization of a high threshold potassium channel in the rat cochlear nucleus. J Comp Neurol 386:178–202.

Postlethwaite M, Hennig MH, Steinert JR, Graham BP, Forsythe ID (2007) Acceleration of AMPA receptor kinetics underlies temperature-dependent changes in synaptic strength at the rat calyx of Held. J Physiol (Lond), in press.

Richardson FC, Kaczmarek LK (2000) Modification of delayed rectifier potassium currents by the Kv9.1 potassium channel subunit. Hear Res 147:21–30.

Rose CR (2002) Na^+ signals at central synapses. Neuroscientist 8:532–539.

Rose CR, Konnerth A (2001) NMDA receptor-mediated Na^+ signals in spines and dendrites. J Neurosci 21:4207–4214.

Rose CR, Ransom BR (1997) Regulation of intracellular sodium in cultured rat hippocampal neurons. J Physiol (Lond) 499:573–587.

Santi CM, Ferreira G, Yang B, Gazula VR, Butler A, Wei A, Kaczmarek LK, Salkoff L (2006) Opposite regulation of Slick and Slack K^+ channels by neuromodulators. J Neurosci 26:5059–5068.

Saviane C, Silver RA (2006) Fast vesicle reloading and a large pool sustain high bandwidth transmission at a central synapse. Nature 439:983–987.

Song P, Yang Y, Barnes-Davies M, Bhattacharjee A, Hamann M, Forsythe ID, Oliver DL, Kaczmarek LK (2005) Acoustic environment determines phosphorylation state of the Kv3.1 potassium channel in auditory neurons. Nat Neurosci 8:1335–1342.

Taschenberger H, von Gersdorff H (2000) Fine-tuning an auditory synapse for speed and fidelity: developmental changes in presynaptic waveform, EPSC kinetics, and synaptic plasticity. J Neurosci 20:9162–9173.

Uchino S, Wada H, Honda S, Hirasawa T, Yanai S, Nakamura Y, Ondo Y, Kohsaka S (2003) Slo2 sodium-activated K^+ channels bind to the PDZ domain of PSD-95. Biochem Biophys Res Commun 310:1140–1147.

Wang L-Y, Gan L, Forsythe ID, Kaczmarek LK (1998) Contribution of the Kv3.1 potassium channel to high-frequency firing in mouse auditory neurons. J Physiol (Lond) 509:183–194.

Wang Z, Kimitsuki T, Noma A (1991) Conductance properties of the Na^+-activated K^+ channel in guinea-pig ventricular cells. J Physiol (Lond) 433:241–257.

Wu SH, Kelly JB (1993) Response of neurons in the lateral superior olive and medial nucleus of the trapezoid body to repetitive stimulation: intracellular and extracellular recordings from mouse brain slice. Hear Res 68:189–201.

Yang B, Gribkoff VK, Pan J, Damagnez V, Dworetzky SI, Boissard CG, Bhattacharjee A, Yan Y, Sigworth FJ, Kaczmarek LK (2006) Pharmacological activation and inhibition of *Slack* (*Slo*2.2) channels. Neuropharmacology 51:896–906.

Yuan A, Santi CM, Wei A, Wang Z-W, Pollak K, Nonet M, Kaczmarek LK, Crowder CM, Salkoff L (2003) The sodium-activated potassium channel is encoded by a member of the *Slo* gene family. Neuron 37:765–773.

Zhong N, Beaumont V, Zucker RS (2001) Roles for mitochondrial and reverse mode Na^+/Ca^{2+} exchange and the plasmalemma Ca^{2+} ATPase in post-tetanic potentiation at crayfish neuromuscular junctions. J Neurosci 21:9598–9607.